Graphene-Supported Palladium Complex: A Highly Efficient, Robust and Recyclable Catalyst for the Suzuki–Miyaura Cross-Coupling of Various Aryl Halides

Abu Taher
Dong-Jin Lee
Ik-Mo Lee*

Department of Chemistry, Inha University, Incheon 402-751,
Republic of Korea
imlee@inha.ac.kr

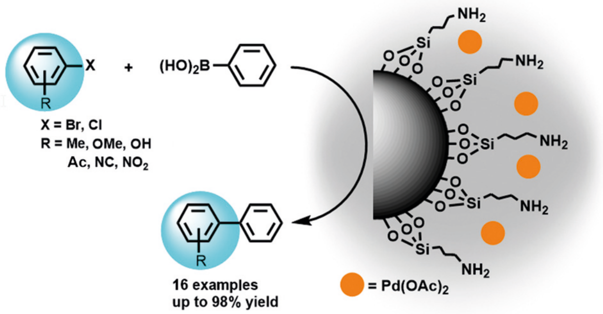

Received: 02.06.2016
Accepted after revision: 30.06.2016

DOI: 10.1055/s-0035-1562607; Art ID: st-2016-u0378-l

Abstract We present a novel strategy based on the immobilization of a palladium complex on reduced graphene oxide for the development of a heterogeneous catalytic system with high efficiency and good recyclability. The prepared catalyst was tested for Suzuki–Miyaura cross-coupling reactions and shown to have a high catalytic efficiency, giving 83−98% conversion of the reactants under mild conditions. Moreover, it could be readily recycled and reused several times without significant loss of activity.

Key words graphene oxide, Suzuki coupling, heterogeneous catalysis, palladium catalysis, catalyst support, aryl halides

The impact of metal-catalyzed coupling reactions in the preparation of natural products, pharmaceuticals, and molecular organic compounds has been widespread.[1,2] In this context, palladium-catalyzed C–C bond-formation reactions are among the most efficient techniques in organic synthesis.[3] In particular, the Suzuki–Miyaura cross-coupling reaction has served as an innovative pathway for the construction of biaryl units.[4,5] Homogeneous metal catalysts are frequently used in coupling reactions,[6] and the immobilization of homogeneous metal catalysts onto solid supports is one of the major challenges in the field of catalysis. In addition, recyclability of homogeneous metal catalysts is considered a major objective in relation to green chemistry.[7] One approach to such an environmentally benign process is based on the development of supported catalysts that exhibit extremely high catalytic activities, even in aqueous media.[8] Thus, efforts have been made to immobilize homogeneous catalysts on diverse support materials, such as nanoparticles,[9] inorganic solids,[10] polymers,[11] dendrimers,[12] or perfluorinated tags.[13]

Graphene[14] and reduced graphene oxide (rGO)[15,16] surfaces have recently gained much attention as convenient supports in heterogeneous catalysis due to their unique two-dimensional structures, huge surface areas, and other excellent properties.[17,18] In fact, these materials have been shown to be promising supports for many metallic nanocatalysts, such as Pd,[19–21] Pd–Ag nanorings,[22] Au,[23] Au–Pt core–shell nanoparticles,[24] or Fe_3O_4.[25] Despite impressive recent improvements in the scope of catalytic reactions, the catalytic protocol still suffers from some disadvantages, such as metal leaching and low reactivities for several important substrate classes, resulting in low yields. Therefore, the development of a reusable catalyst for cross-coupling reactions under mild conditions is highly desirable and is a hot topic in both green chemistry and current organic synthesis. Here, we report a highly efficient method for the immobilization of Pd complexes on rGO as a reusable catalyst for cross-coupling reactions in ethanol–water under mild conditions (Scheme 1).

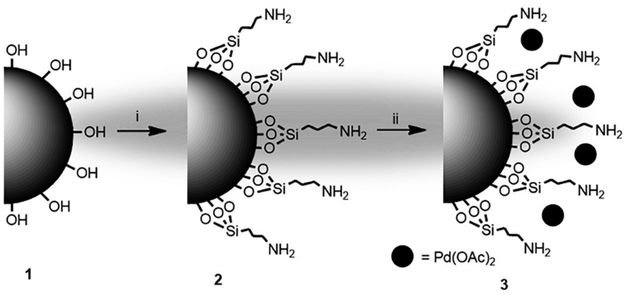

Scheme 1 Preparation of graphene-supported palladium complex **3**. *Reagents and conditions*: (i) [3-(triethoxysilyl)propyl]amine, toluene, 100 °C, 10 h. (ii) $Pd(OAc)_2$, acetone, 45 °C, 12 h.

Amine-functionalized rGO **2** was prepared from commercially available rGO (**1**) by treatment with [3-(triethoxysilyl)propyl]amine (APL) in toluene with mild sonication for 10 minutes and then heating to 100 °C for ten hours. Treatment of **2** with $Pd(OAc)_2$ in acetone at 45 °C for 12 hours, followed by filtration and repeated washing with excess CH_2Cl_2 at room temperature gave the catalyst **3** containing immobilized Pd complexes (Scheme 1). The palladium complexes were encapsulated within the amine-functionalized rGO layer through coordination,[15a] and the nature of these complexes was examined by Fourier-transform IR spectroscopy, field-emission transmission electron microscopy (FE-TEM), high-resolution scanning electron microscopy (SEM); X-ray photoelectron spectroscopy (XPS), energy-dispersive X-ray spectroscopy (EDS), thermogravimetric analysis (TGA), inductively coupled plasma (ICP) analysis, and Raman spectroscopy. The amount of immobilized Pd in catalyst **3** was determined by ICP analysis to be 5.75%, which exactly matched the calculated value. The morphology of **3** was studied by TEM and SEM. Figure 1 (a and b) shows TEM images of fresh and recycled samples of catalyst **3**. SEM and the corresponding elemental mapping by EDS analysis of **3** showed that palladium was homogeneously distributed in the hybrid material [Figure 1 (d)]. Figure 1 (e) shows typical FTIR spectra of **1**, **2**, and **3**. rGO **1** showed typical absorption features that included coupled C–O stretching vibrations at 1058 cm^{-1}, O–H bending vibrations at 1458 cm^{-1}, C=O stretching vibrations at 1718 cm^{-1}, CH_2 stretching vibrations at 2853 and 2921 cm^{-1}, CH_3 stretching vibrations at 2968 cm^{-1}, and O–H stretching vibrations at 3434 cm^{-1}.[26–29] The vibration at 3434 cm^{-1} was attributed to absorbed water.[26] After silanization, the apparent increases in intensity at 1060 and 2921 cm^{-1} are direct evidence of Si–O stretching and the presence of methylene groups from the silicon coupling agent APL, respectively [Figure 1 (e); center]. Subsequently, on treatment with $Pd(OAc)_2$, the C–H peak increased in intensity and a new peak appeared at 1718 cm^{-1}, which was assigned to the carbonyl group [Figure 1 (e); bottom].[28,29] This peak confirmed the presence of $Pd(OAc)_2$ on the surface of **2**. However, an intense broad band associated with hydroxy groups[26] remained, due to small solvent molecules adsorbed on the surface of the graphene flakes or inserted between layers during sonication.[30]

Raman spectroscopy is a convenient and powerful tool for probing the structure of graphene-based materials. Figure 1 (f) shows the featured regions of the Raman spectra for **1**, **2** and **3**. In all the Raman spectra, two dominant peaks for the D and G bands were observed at around 1308 and 1595 cm^{-1}, respectively.[29,31,32] The D band is due to the breathing mode of the *K* point phonons of A_{1g} symmetry, and the G band corresponds to first-order scattering of the E_{2g} phonons. The constant position of the G band at 1595 cm^{-1} across the whole supported area of the samples indicates that the strain and doping are homogeneous.[33] After silanization of **1**, the I(D)/I(G) ratio of the silanized graphene increased rapidly from 1.30 to 1.41. This is due to a decrease in the average size of the in-plane sp^2 domains upon silanization.[26] For **3**, the I(D)/I(G) ratio was drastically decreased to 1.34, indicative of an increasing order of formation of $Pd(OAc)_2$ onto **2**. The spectrum [Figure 1 (f); bottom] shows an additional peak at around 432 cm^{-1} due to the presence of palladium.[34] Moreover, the EDX spectra confirmed the presence of palladium on the rGO surface (see Supporting Information, Figure S1).

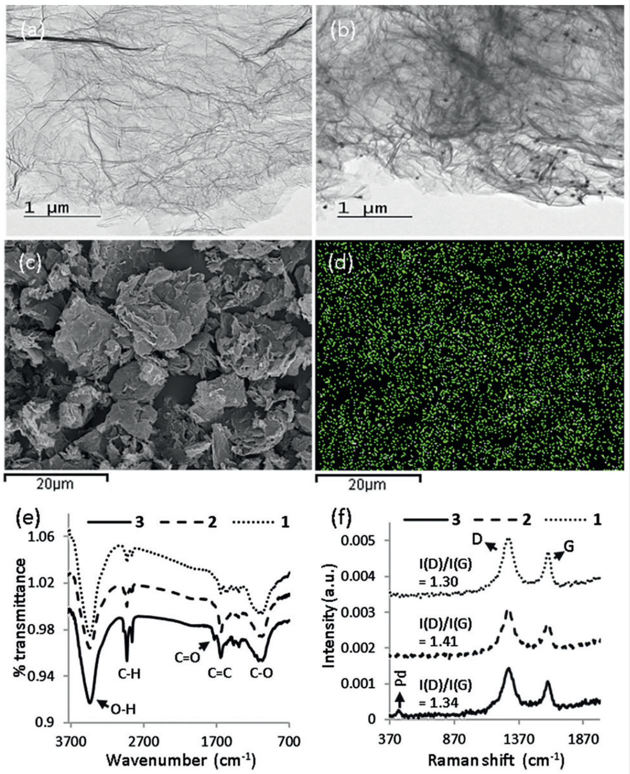

Figure 1 TEM images of catalyst **3** (a) before use and (b) after a fifth catalytic run; (c) SEM image of **3**; (d) corresponding quantitative EDS mapping of Pd; (e) FTIR spectra and (f) Raman spectra of **1**, **2**, and **3**. The corresponding I(D)/I(G) values are indicated for each spectrum.

The chemical compositions of the as-prepared **3** complexes were determined by means of TGA. Figure S2 (Supporting Information) shows typical TGA curves for samples of **1**, **2**, and **3**. rGO materials are not thermally stable, and mass loss started below 100 °C and was rapid at 150 °C.[35] Mass loss between 350 °C and 750 °C was assigned to burning of graphitic carbon.[36] The TGA curve for **3** showed a 12% mass loss below 250 °C, which corresponded to loss of water and trace amounts of oxygen.[36] At temperatures up to 800 °C, total weight losses of 9, 19, and 33 wt% were observed for **1**, **2**, and **3**, respectively. We assume that the weight loss that occurred during thermal decomposition of

3 was due to palladium moieties. Furthermore, the results of TGA also indicated that the graphene-supported catalyst **3** has excellent thermal stability.

To gain further insights into surface changes associated with the chemical reaction shown in Scheme 1, we performed XPS measurements. As expected, only C 1s and O 1s peaks were seen in the XPS spectrum for **1** [Figure 2 (a); insert]. The appearance of the Si 2s (152 eV), Si 2p (101 eV), and N 1s (399.5 eV) peaks accompanying the C 1s and O 1s peaks in the XPS spectrum of **2** [Figure 2 (a)] confirmed that APS was covalently bonded to **1**.[26,37] The N 1s spectrum is very useful for analyzing the nature of N functionalities. The N 1s spectrum of **2** can be deconvoluted into three components at 399.17, 400.04, and 400.89 eV, corresponding to C–NH_2, N–H, and NH_2, respectively [Figure 2 (c)].[38,39] A new peak for C–N (285.4 eV) in **2** confirmed the presence of amino groups (Supporting Information, Figure S3a). Furthermore, the O 1s spectrum could be reasonably fitted by a single peak at 531.68 eV, indicating a high purity for product **2** (Supporting Information; Figure S3b). The XPS survey spectrum of **3** showed the adsorption of palladium onto **2** [Figure 2 (b)]. Furthermore, the presence of the Pd 3d3/2 (343.13 eV) and Pd 3d5/2 (337.60 eV) peaks indicated successful coordination bonding of $Pd(OAc)_2$ onto **2** [Figure 2 (d)].[40,41]

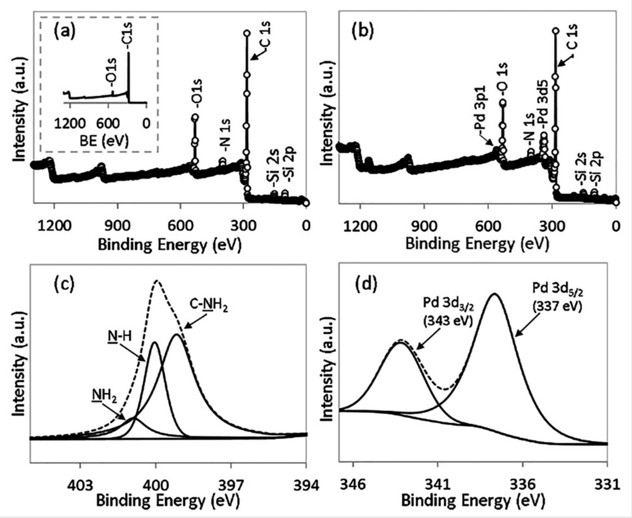

Figure 2 XPS spectra of **1** [a (insert)], **2** (a), and **3** (b); High-resolution XPS spectra of N1s for **2** (c) and Pd 3d for **3** (d).

The Suzuki–Miyaura cross-coupling reaction is one of the most significant reactions for the construction of biaryl units in organic synthesis,[42] and various Pd catalysts have been used for this reaction.[43] Aryl iodides have been employed as suitable coupling substrates in most coupling reactions with arylboronic acids. However, the use of inexpensive aryl bromides or chlorides would be highly desirable for large-scale applications. Furthermore, recycling and recovery of catalysts have been problematic in relation to the production of fine chemicals. Initially, we examined the Suzuki–Miyaura cross-coupling of 2-bromotoluene with phenylboronic acid in the presence of various amounts of catalyst **3** to determine the optimal loading. As shown in Figure 3 (a), the yield of the reaction gradually increased with increasing catalyst loading in the range 0.01–0.2 mol%. A high catalytic activity was still observed at a low catalyst loading. Whereas the reaction yield reached almost 100% conversion with 0.16 mol% of **3**, 0.2 mol% of **3** gave a quantitative yield at 80 °C in ethanol–water. Therefore, a 0.2 mol% loading of **3** was determined to be the optimal loading under the reaction conditions.

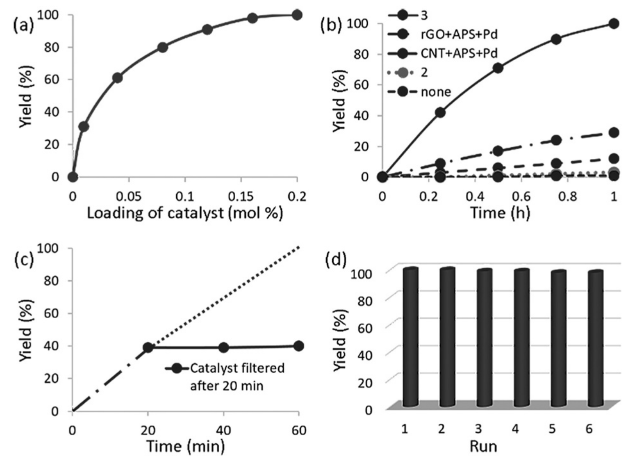

Figure 3 Suzuki–Miyaura cross-coupling of 2-bromotoluene with phenylboronic acid in 1:1 ethanol–water catalyzed by **3**. (a) Effect of various catalyst loadings; (b) comparative catalytic study for **3**, rGO + APS + $Pd(OAc)_2$, MWCNTs + APS + $Pd(OAc)_2$, **2**, and in the absence of catalyst (top to bottom, respectively) with the same catalyst loading (0.2 mol% Pd); (c) hot filtration test; and (d) recyclability test. In all cases the reaction conditions were the same as those in Table 2, entry 2.

Next, various solvents were screened to improve the efficiency of the Suzuki–Miyaura cross-coupling reaction (Table 1). Water alone was a poor solvent (Table 1, entry 1), requiring a long reaction time. The results showed that 1:1 ethanol–water was the best solvent in terms of the catalytic activity (entries 1–4). Next we screened various bases in 1:1 ethanol–water (entries 2 and 5–10) and we found that relatively inexpensive K_2CO_3 gave the best result (entry 2), whereas other inorganic bases showed moderate activities (entries 5–7) and organic bases showed low activities (entries 8–10).

After successfully screening the cross-coupling reaction, we carried out Suzuki–Miyaura reactions of several nonactivated aryl bromides and chlorides. Catalyst **3** maintained a high catalytic reactivity for bromobenzene and nonactivated 2-bromotoluene, 4-bromotoluene, 2-bromoanisole, 4-bromoanisole and 4-bromophenol (Table 2, entries 1–6). The activated aryl bromides 1-bromo-3-nitrobenzene, 1-bromo-4-nitrobenzene, 4-bromoacetophenone, and 1-bro-

Table 1 Optimization of Solvent and Base for Suzuki–Miyaura Cross-Coupling Reaction of 2-Bromotoluene with Phenylboronic Acid Catalyzed by **3**[a]

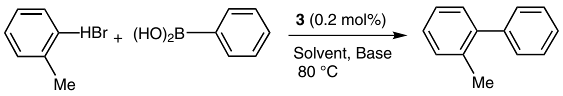

Entry	Solvent	Base	Time (h)	Yield[b] (%)
1	H_2O	K_2CO_3	6	94 (91)
2	1:1 EtOH–H_2O	K_2CO_3	1	100 (98)
3	1:1 DMF–H_2O	K_2CO_3	3.5	81
4	1:1 1,4-dioxane–H_2O	K_2CO_3	3	86
5	1:1 EtOH–H_2O	K_3PO_4	1	86 (85)
6	1:1 EtOH–H_2O	Na_2CO_3	1	81 (78)
7	1:1 EtOH–H_2O	KOAc	1	58
8	1:1 EtOH–H_2O	Et_3N	1	51
9	1:1 EtOH–H_2O	piperazine	1	35
10	1:1 EtOH–H_2O	Et_2NH	1	trace

[a] Reaction conditions: 2-bromotoluene (1.0 mmol), $PhB(OH)_2$ (1.2 mmol), base (2.0 mmol), solvent (3.5 mL), 80 °C.
[b] GC yields; isolated yields are given in parentheses.

Table 2 Suzuki–Miyaura Cross-Coupling of Aryl Halides with $PhB(OH)_2$ in Ethanol–Water[a]

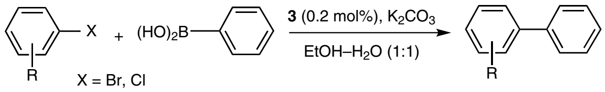

Entry	R	X	Time (h)	Yield[b] (%)
1	H	Br	0.6	96
2	2-Me	Br	1	98
3	4-Me	Br	1	95
4	2-MeO	Br	0.6	97
5	4-MeO	Br	0.6	98
6	4-HO	Br	0.6	95
7	3-O_2N	Br	0.5	97
8	4-O_2N	Br	0.5	98
9	4-Ac	Br	0.5	98
10	4-NC	Br	0.6	96
11[c]	4-Ac	Br	4	98
12[c]	3-O_2N	Br	4	96
13[d]	2,6-Me_2	Cl	3	88
14[d]	H	Cl	7	96
15[d]	2-Me	Cl	7	92
16[d]	4-HO	Cl	7	83

[a] Reaction conditions: aryl halide (1.0 mmol), $PhB(OH)_2$ (1.2 mmol), K_2CO_3 (2.0 mmol), 1:1 EtOH–H_2O (3.5 mL), 80 °C.
[b] Isolated yield.
[c] At r.t.
[d] At 90 °C.

mo-4-isocyanobenzene rapidly gave the corresponding coupling products in quantitative yields (entries 7–10). The cross-coupling reactions of two bromides with electron-withdrawing aryl groups, 4-bromoacetophenone and 1-bromo-3-nitrobenzene, were efficiently promoted, even at room temperature, giving the corresponding products in almost quantitative yields (entries 11 and 12). As expected, aryl bromides with electron-withdrawing groups showed somewhat higher reactivities than those with electron-donating groups. Sterically hindered 2,5-dimethylbromobenzene also efficiently coupled with phenylboronic acid to give the coupling product in 88% yield (entry 13). It is notable that catalyst **3** also smoothly promoted the Suzuki–Miyaura reaction of aryl chlorides with phenylboronic acid to provide the corresponding coupling products in up to 96% yield (entries 14–16). These results demonstrate that catalyst **3** successfully promotes the coupling reactions of various aryl bromides or chlorides with either electron-withdrawing or electron-donating substituents under mild conditions.

A control experiment carried out under exactly the same conditions showed that **2** was ineffective as a catalyst, as it gave similar results to those obtained in the absence of a catalyst [Figure 3 (b)]. When a mixture of rGO, APS, and Pd(OAc) or a mixture of multiwall carbon nanotubes (MWCNTs), APS, and $Pd(OAc)_2$ was used, a relatively poor yield was obtained. Reports in the literature suggest that this might be due to the absence of coordinating ligands.[15a] On the other hand, the supported catalyst **3** gave a quantitative yield under the same reaction conditions. These result demonstrate that the presence of connecting ligands between the rGO and Pd moieties promotes the catalytic reaction in the Suzuki–Miyaura cross-coupling.

Next, we turned our attention to testing the reusability of the catalyst under mild conditions. A critical issue with a heterogeneous catalyst is the possibility that a proportion of the active molecules can migrate from the solid to the liquid phase by leaching. The leached molecules might then be responsible for a significant proportion of the catalytic activity. To test this possibility, two identical reactions of 2-bromotoluene with phenylboronic acid were carried out with continuous monitoring of the conversion after 20 minutes. One reaction was carried out in the presence of the catalyst until the conversion reached 39% and then the solids were removed from the reaction mixture by filtration. The liquid phase was then transferred to a new reaction vial and allowed to react further, but no significant change in conversion was observed [Figure 3 (c)]; after one hour, the conversion was 40%, indicating that no active species was present in the reaction vial.

The reusability of the catalyst was also examined. A major advantage of the catalyst is that it can be easily recovered by simple filtration. The recycling of the catalyst was examined in the coupling of 2-bromotoluene with phenylboronic acid in 1:1 ethanol–water [Figure 3 (d)]. Similar yields (100% to 98%) were obtained over the six runs, without any significant loss of activity. The possible leaching of Pd after completion of the reaction was monitored by ICP-MS, which showed a total loss of 0.7 wt%. A comparative TEM study of the catalyst **3** before and after the experiments [Figure 1 (a and b)] showed that Pd nanoparticles were dispersed on the rGO after several reaction runs. The results of this study agreed with reports in the literature that the formation of Pd nanoparticles on the rGO surface as an active species developed during the reaction.[45,46] The extremely high stability and reusability of the prepared catalyst might be due to the strong interactions between rGO and the Pd moieties, which promote the catalytic reaction under mild conditions.

In conclusion, we have designed and developed a highly active heterogeneous palladium catalyst supported on reduced graphene oxide for coupling reactions in ethanol–water. We showed that the catalyst could be used to couple a wide range of less reactive aryl halides with phenylboronic acid under mild conditions. Repeated reactions performed by using a recycled catalyst showed similar yields without a significant loss in activity. Advantages of the present method include simple workups, high yields, and good recyclability of the catalyst.

Acknowledgment

This work was supported by an Inha University Research Grant (Inha 2014).

Supporting Information

Supporting information for this article is available online at http://dx.doi.org/10.1055/s-0035-1562607.

References and Notes

(1) Wang, S.; Li, J.; Miao, T.; Wu, W.; Li, Q.; Zhuang, Y.; Zhou, Z.; Qiu, L. *Org. Lett.* **2012**, *14*, 1966.
(2) Shukla, S. P.; Tiwari, R. K.; Verma, A. K. *J. Org. Chem.* **2012**, *77*, 10382.
(3) Keske, E. C.; Zenkina, O. V.; Wang, R.; Crudden, C. M. *Organometallics* **2012**, *31*, 6215.
(4) Banwell, M. G.; Goodwin, T. E.; Ng, S.; Smith, J. A.; Wong, J. D. *Eur. J. Org. Chem.* **2006**, 3043.
(5) Kotha, S.; Lahiri, K. *Eur. J. Org. Chem.* **2007**, 1221.
(6) Lee, D.-H.; Jin, M.-J. *Org. Lett.* **2011**, *13*, 252.
(7) Cole-Hamilton, D. J. *Science* **2003**, *299*, 1702.
(8) Herrmann, W. A.; Kohlpaintner, C. W. *Angew. Chem.* **1993**, *105*, 1588.
(9) (a) Taher, A.; Kim, J.-B.; Jung, J.-Y.; Ahn, W.-S.; Jin, M.-J. *Synlett* **2009**, 2477. (b) Wittmann, S.; Schätz, A.; Grass, R. N.; Stark, W. J.; Reiser, O. *Angew. Chem. Int. Ed.* **2010**, *49*, 1867.
(10) (a) Paul, S.; Clark, J. H. *Green Chem.* **2003**, *5*, 635. (b) Horniakova, J.; Raja, T.; Kubota, Y.; Sugi, Y. *J. Mol. Catal. A: Chem.* **2004**, *217*, 73.
(11) Uozumi, Y. *Bull. Chem. Soc. Jpn.* **2008**, *81*, 1183.
(12) Andrés, R.; de Jesús, E.; Flores, J. C. *New J. Chem.* **2007**, *31*, 1161.
(13) Garcia-Bernabé, A.; Tzschucke, C. C.; Bannwarth, W.; Haag, R. *Adv. Synth. Catal.* **2005**, *347*, 1389.
(14) Liu, K.; Chen, T.; Hou, Z.; Wang, Y.; Dai, L. *Catal. Lett.* **2014**, *144*, 314.
(15) (a) Bai, C.; Zhao, Q.; Li, Y.; Zhang, G.; Zhang, F.; Fan, X. *Catal. Lett.* **2014**, *144*, 1617. (b) Chua, C. K.; Pumera, M. *Chem. Soc. Rev.* **2014**, *43*, 291.
(16) Meyer, J. C.; Geim, A. K.; Katsnelson, M. I.; Novoselov, K. S.; Booth, T. J.; Roth, S. *Nature* **2007**, *446*, 60.
(17) Dreyer, D. R.; Park, S.; Bielawski, C. W.; Ruoff, R. S. *Chem. Soc. Rev.* **2010**, *39*, 228.
(18) Tan, R.; Li, C.; Luo, J.; Kong, Y.; Zheng, W.; Yin, D. *J. Catal.* **2013**, *298*, 138.
(19) Morimoto, N.; Yamamoto, S-i.; Takeuchi, Y.; Nishina, Y. *RSC. Adv.* **2013**, *3*, 15608.
(20) Santra, S.; Hota, P. K.; Bhattacharyya, R.; Bera, P.; Ghosh, P.; Mandal, S. K. *ACS. Catal.* **2013**, *3*, 2776.
(21) Shang, N.; Feng, C.; Zhang, H.; Gao, S.; Tang, R.; Wang, C.; Wang, Z. *Catal. Commun.* **2013**, *40*, 111.
(22) Liu, M.; Lu, Y.; Chen, W. *Adv. Funct. Mater.* **2013**, *23*, 1289.
(23) Qin, Y.; Li, J.; Kong, Y.; Li, X.; Tao, Y.; Li, S.; Wang, Y. *Nanoscale* **2014**, *6*, 1281.
(24) Qi, J.; Lv, W.; Zhang, G.; Li, Y.; Zhang, G.; Zhang, F.; Fan, X. *Nanoscale* **2013**, *5*, 6275.
(25) Feng, C.; Zhang, H.-Y.; Shang, N.-Z.; Gao, S.-T.; Wang, C. *Chin. Chem. Lett.* **2013**, *24*, 539.
(26) Nie, Y.; Hübert, T. *Polym. Int.* **2011**, *60*, 1574.
(27) Zhan, Y.; Wu, J.; Xia, H.; Yan, N.; Fei, G.; Yuan, G. *Macromol. Mater. Eng.* **2011**, *296*, 590.
(28) Huang, K.-J.; Niu, D.-J.; Liu, X.; Wu, Z.-W.; Fan, Y.; Chang, Y.-F.; Wu, Y.-Y. *Electrochim. Acta* **2011**, *56*, 2947.
(29) Pham, V. H.; Cuong, T. V.; Hur, S. H.; Oh, E.; Kim, E. J.; Shin, E. W.; Chung, J. S. *J. Mater. Chem.* **2011**, *21*, 3371.
(30) Zhang, X.; Wan, S.; Pu, J.; Wang, L.; Liu, X. *J. Mater. Chem.* **2011**, *21*, 12251.
(31) Stankovich, S.; Dikin, D. A.; Piner, R. D.; Kohlhaas, K. A.; Kleinhammes, A.; Jia, Y.; Wu, Y.; Nguyen, S. T.; Ruoff, R. S. *Carbon* **2007**, *45*, 1558.
(32) Wang, H.; Robinson, J. T.; Li, X.; Dai, H. *J. Am. Chem. Soc.* **2009**, *131*, 9910.
(33) Tiberj, A.; Rubio-Roy, M.; Paillet, M.; Huntzinger, J.-R.; Landois, P.; Mikolasek, M.; Contreras, S.; Sauvajol, J.-L.; Dujardin, E.; Zahab, A.-A. *Sci. Rep.* **2013**, *3*, 2355.
(34) Parambhath, V. B.; Nagar, R.; Sethupathi, K.; Ramaprabhu, S. *J. Phys. Chem. C* **2011**, 115–15679.
(35) Fang, M.; Wang, K.; Lu, H.; Yang, Y.; Nutt, S. *J. Mater. Chem.* **2009**, *19*, 7098.
(36) Rakhi, R. B.; Chen, W.; Cha, D.; Alshareef, H. N. *J. Mater. Chem.* **2011**, *21*, 16197.
(37) Xue, Y.; Liu, Y.; Lu, F.; Qu, J.; Chen, H.; Dai, L. *J. Phys. Chem. Lett.* **2012**, *3*, 1607.
(38) Yang, D.; Velamakanni, A.; Bozoklu, G.; Park, S.; Stoller, M.; Piner, R. D.; Stankovich, S.; Jung, I.; Field, D. A.; Ventris, C. A. Jr.; Ruoff, R. S. *Carbon* **2009**, *47*, 145.

(39) Wang, M.; Zhao, Y.; Xu, R.; Zhang, M.; Fu, R. K. Y.; Chu, P. K. *Diamond Relat. Mater.* **2013**, *38*, 28.

(40) Siamaki, A. R.; Lin, Y.; Woodberry, K.; Connell, J. W.; Gupton, B. F. *J. Mater. Chem. A* **2013**, *1*, 12909.

(41) Brun, N.; Hesemann, P.; Laurent, G.; Sanchez, C.; Birot, M.; Deleuze, H.; Backov, R. *New J. Chem.* **2013**, *37*, 157.

(42) (a) Phan, N. T. S.; Van Der Sluys, M.; Jones, C. W. *Adv. Synth. Catal.* **2006**, *348*, 609. (b) Molander, G. A.; Canturk, B. *Angew. Chem. Int. Ed.* **2009**, *48*, 9240. (c) Milde, B.; Schaarschmidt, D.; Rüffer, T.; Lang, H. *Dalton Trans.* **2012**, *41*, 5377.

(43) (a) Lee, D.-H.; Jung, J.-Y.; Lee, I.-M.; Jin, M.-J. *Eur. J. Org. Chem.* **2008**, 356. (b) Taher, A.; Kim, J.-B.; Jung, J.-Y.; Ahn, W.-S.; Jin, M.-J. *Synlett* **2009**, 2477. (c) Zhang, Q.; Su, H.; Luo, J.; Wei, Y. *Catal. Sci. Technol.* **2013**, *3*, 235.

(44) **Suzuki–Miyaura Reaction; General Procedure**
The appropriate aryl halide (1.0 mmol), PhB(OH)$_2$ (1.2 mmol), K_2CO_3 (2.0 mmol), and catalyst **3** (0.2 mol%) were heated in 1:1 EtOH–H_2O (3.5 mL). When the reaction was complete, the mixture was diluted with H_2O and CH_2Cl_2. The organic layer was separated, dried ($MgSO_4$), and concentrated under reduced pressure. The crude product was purified by column chromatography on silica gel. As all of the products are known, characterization was by comparison of their ^{1}H and ^{13}C NMR spectra with literature data.

(45) Sabater, S.; Mata, J. A.; Peris, E. *ACS Catal.* **2014**, *4*, 2038.

(46) Movahed, S. K.; Esmatpoursalmani, R.; Bazgir, A. *RSC Adv.* **2014**, *4*, 14586.